

BACKGROUND

Ensemble Kalman filters suffer from sampling errors mainly due to small ensemble sizes. Sampling errors often cause: [1] Variance underestimation, [2] Rank deficient covariances ($N \ll N_x$) and [3] Noisy and spurious correlations. Strategies to reduce/mitigate sampling errors include *localization* and *inflation*:

$$\tilde{x}_i \leftarrow \sqrt{\lambda} (x_i - \bar{x}) + \bar{x}, \quad \hat{\sigma}^2 = \lambda \frac{1}{N-1} \sum_{i=1}^N (x_i - \bar{x})^2,$$

where $\lambda > 1$ is an inflation factor and $i = 1, 2, \dots, N$. Adaptive prior [Anderson 2009, El Gharamti 2018] and posterior inflation [Zhang et al. 2004, Whitaker and Hamill 2012, El Gharamti 2019] forms exist. Inflation is quite an effective tool for atmospheric and land applications, however, studies have argued that it could cause numerical instabilities for certain applications such as the ocean.

Objective

As a way to avoid numerical instabilities in certain models, is it possible to retain sufficient ensemble spread without the need for excessive inflation?

RANDOMIZED DORMANT EnKF

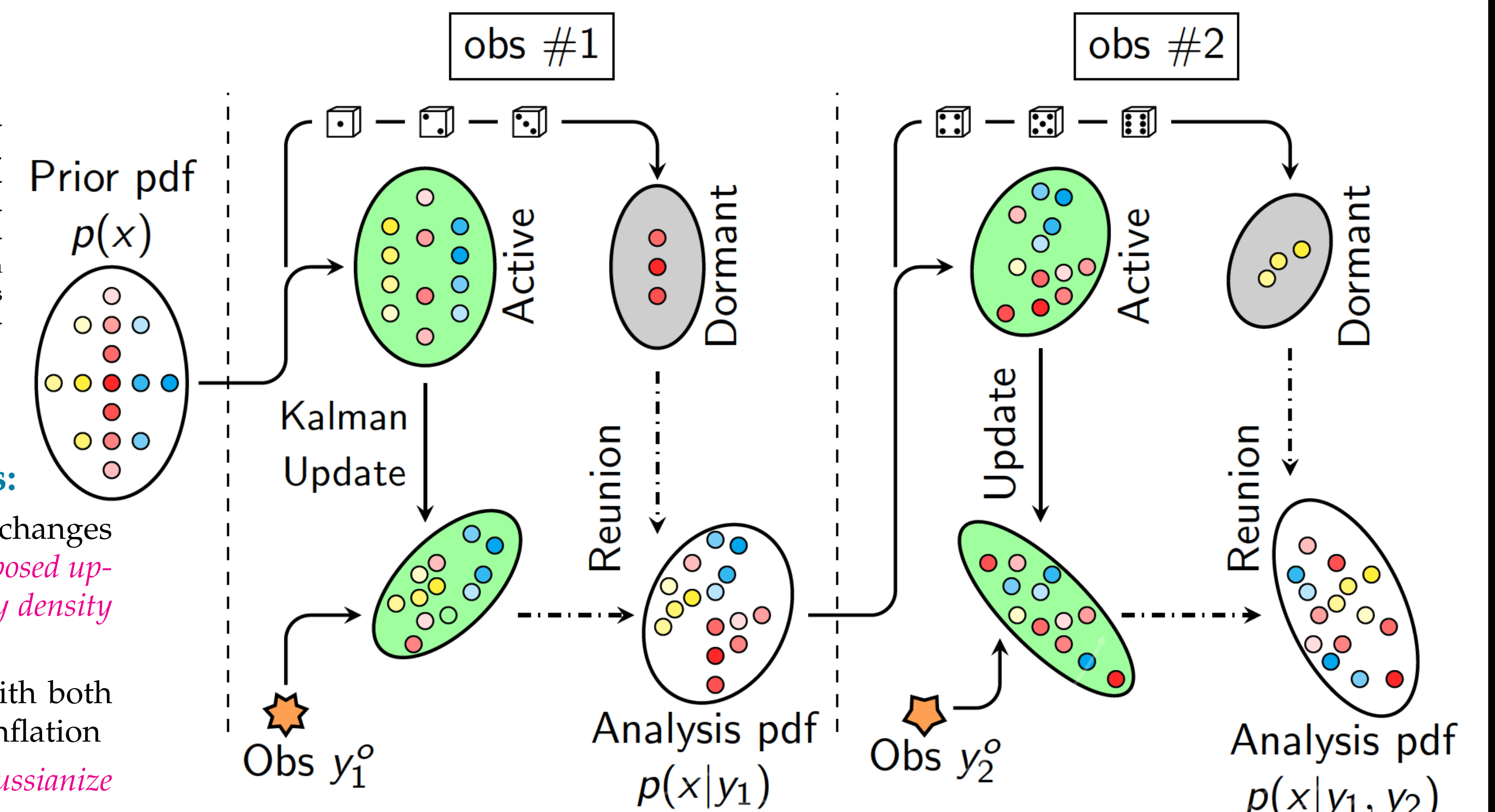
The Randomized Dormant EnKF (RD-EnKF) update step inherently leads to *less spread reduction* than a regular EnKF. The idea is to break down the ensemble each assimilation step into 2 subsets:

1. **Active:** Members within this subset go through a regular EnKF update,

2. **Dormant:** Members (chosen randomly) within this subset just sit and wait, such that:

$$N = N_a + N_d, \quad N_d = \lfloor \alpha N \rfloor \quad \alpha \in [0, 1]$$

where $\lfloor \cdot \rfloor$ denotes the rounding or the nearest integer function and α is the dormancy rate. When the observations are assimilated serially (as in DART), the dormant subset can change for each observation. RD-EnKF cycling procedure is illustrated in Figure 2.



Algorithmic Features:

- Unlike inflation that changes the spread only, *the proposed update affects the probability density function as a whole*
- Remains compatible with both localization and prior inflation
- Update tends to *de-gaussianize* the analysis pdf

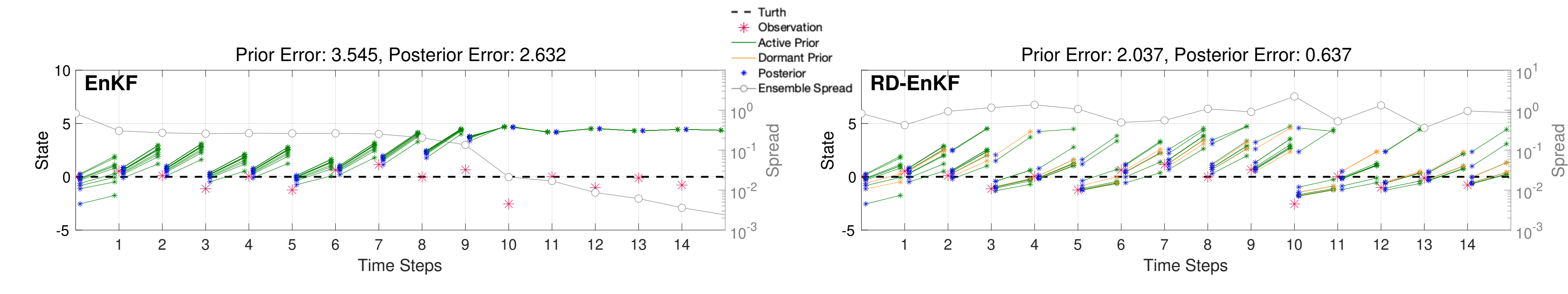


Figure 3: A 1D example from DART's "DART LAB" tutorial illustrating the behavior of the RD-EnKF in a controlled cycling DA system. 10 members are integrated forward in time using a biased nonlinear model. Scalar observations are sampled from the *truth* which is set to 0. The dormancy rate is set to 20% i.e., 2 dormant members (DMs; shown in orange). Overall, the RD-EnKF yields better prior and posterior accuracy than the EnKF while maintaining sufficient spread. The EnKF diverges after ~10 cycles. The evolution of the associated pdfs, using 80 members, in time for each scheme are displayed to the right.

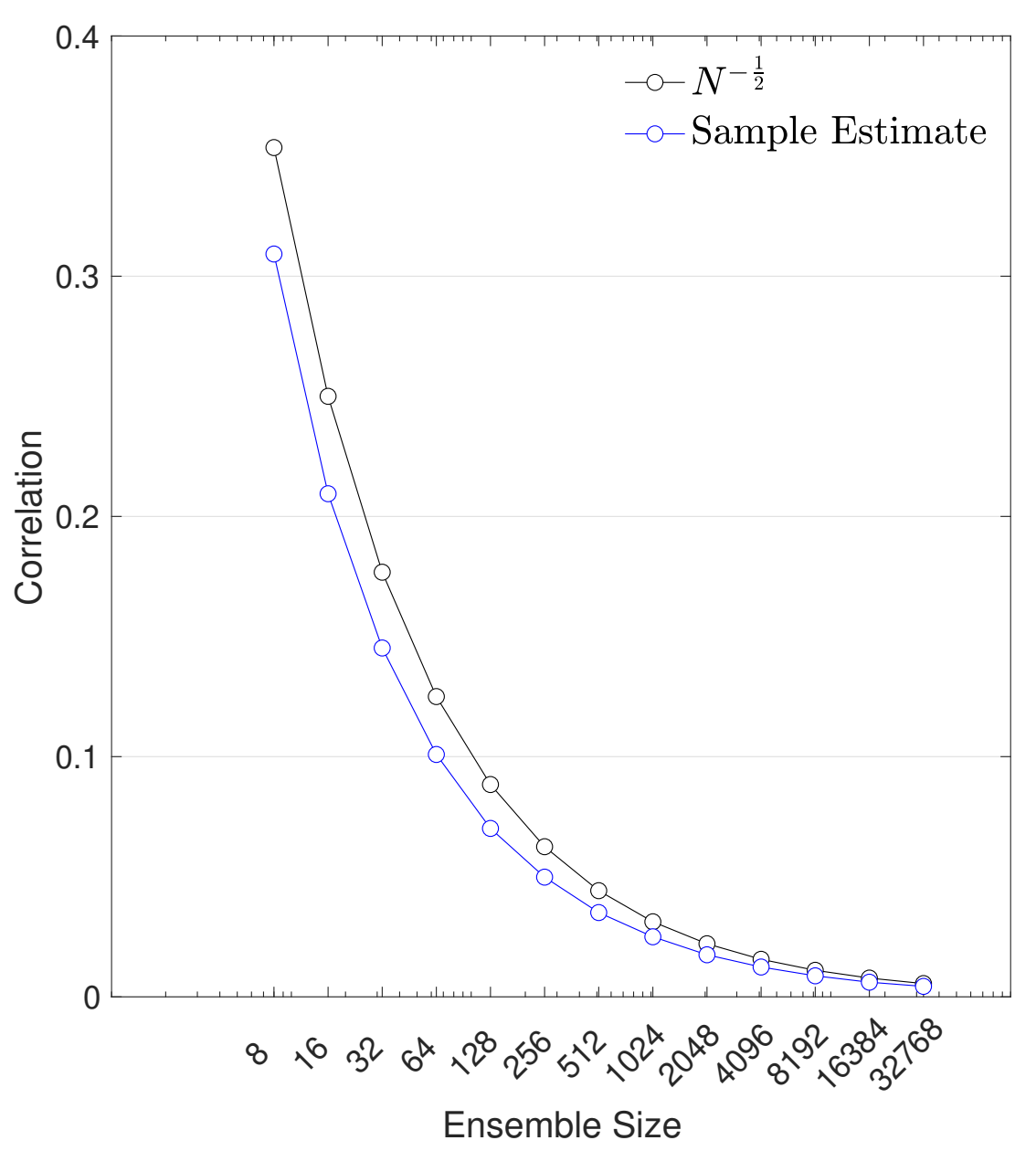


Figure 1: Sample correlation of two independent random variables using random draws with different ensemble sizes. $1/\sqrt{N}$ curve depicts the convergence rate.

LORENZ '96 EXPERIMENTS

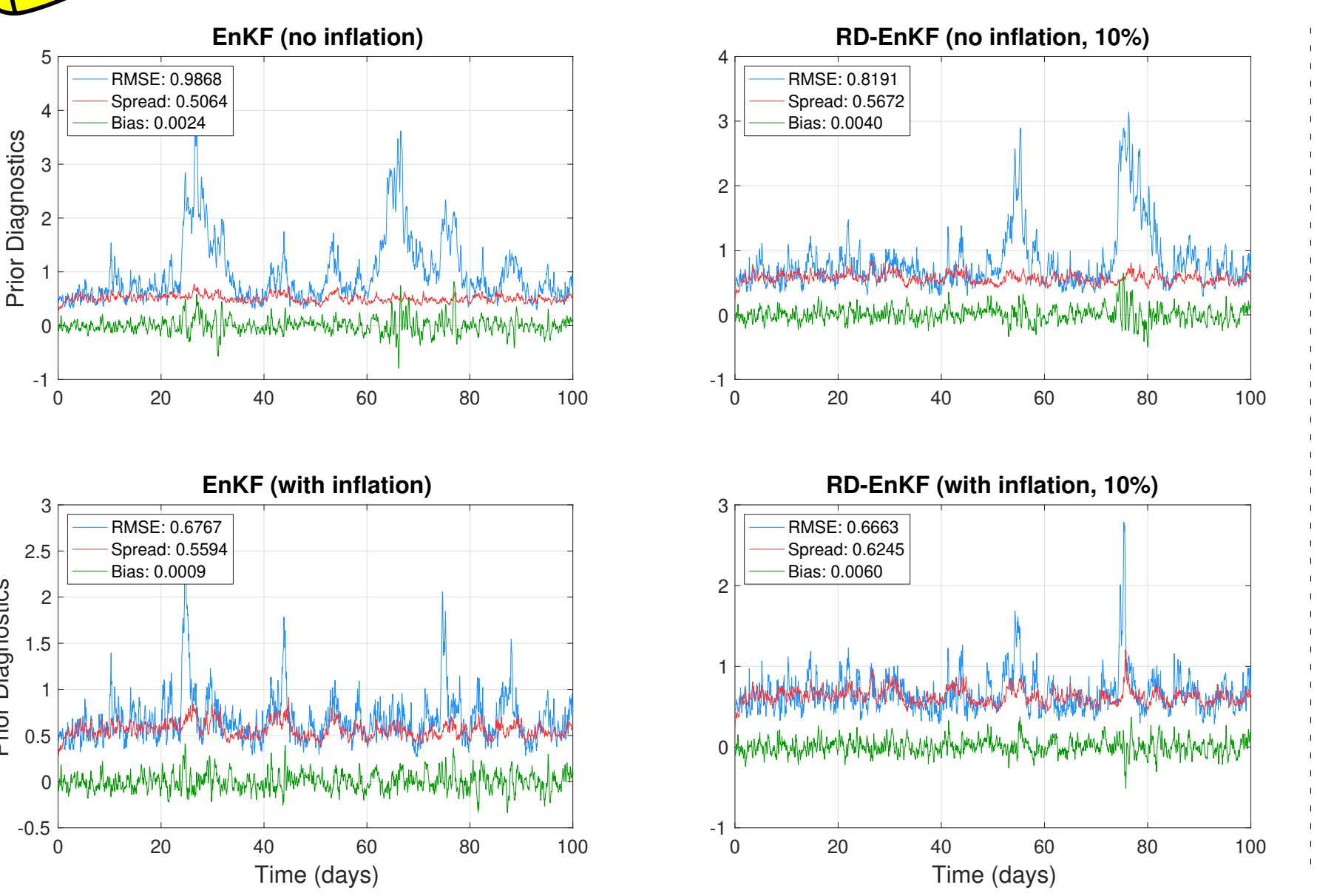


Figure 2: Lorenz '96 experiments showing time-series plots of RMSE, Spread, and Bias for EnKF and RD-EnKF with and without inflation. The left panels show Prior Diagnostics (RMSE, Spread, Bias) vs Time (days). The middle panels show RMSE, Spread, and Bias vs Localization Cutoff (0.1 to 0.3). The right panels show No Inflation and With Adaptive Inflation heatmaps of RMSE vs Ensemble Size (10 to 80) and Localization Cutoff (0.1 to 0.3).

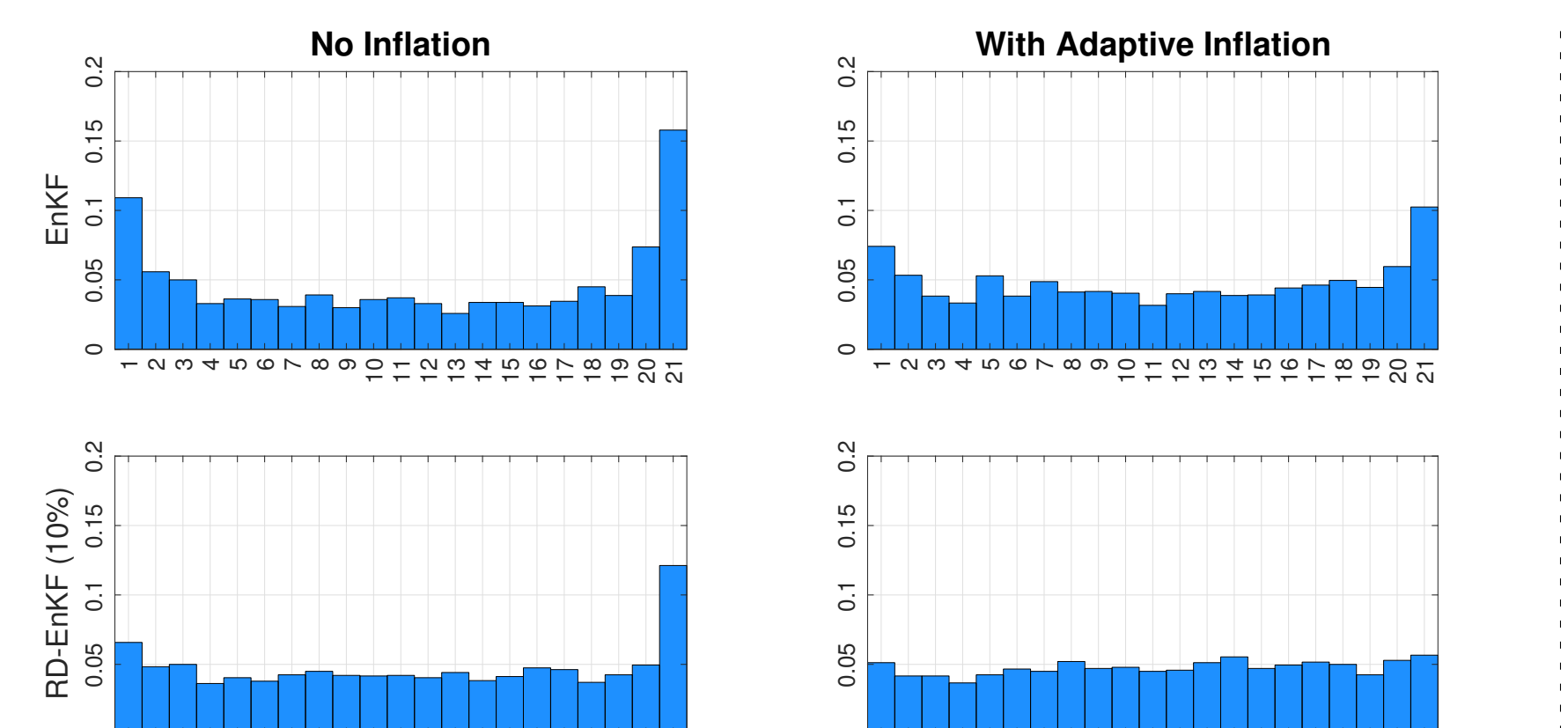


Figure 3: Observing System Simulation Experiments (perfect model) are performed using the L96 model and DART. Cycling is performed every hour using 20 observations distributed evenly throughout the domain. The left panels show time-series plots of RMSE, Spread and Bias of the stochastic EnKF and the RD-EnKF using 20 members. Localization sensitivity runs are shown for both filters in the middle panels. The right panels show the overall RMSE of each scheme using a fixed localization (cutoff is 0.1) and different ensemble sizes.

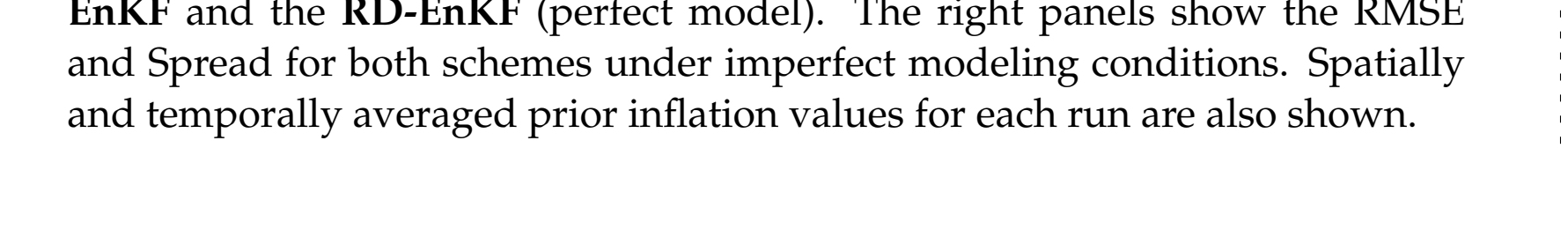


Figure 4: Observing System Simulation Experiments (perfect model) are performed using the L96 model and DART. Cycling is performed every hour using 20 observations distributed evenly throughout the domain. The left panels show time-series plots of RMSE, Spread and Bias of the stochastic EnKF and the RD-EnKF using 20 members. Localization sensitivity runs are shown for both filters in the middle panels. The right panels show the overall RMSE of each scheme using a fixed localization (cutoff is 0.1) and different ensemble sizes.



Figure 5: Rank histograms for unobserved variable #32 obtained using the EnKF and the RD-EnKF (perfect model). The right panels show the RMSE and Spread for both schemes under imperfect modeling conditions. Spatially and temporally averaged prior inflation values for each run are also shown.



Figure 5: Rank histograms for unobserved variable #32 obtained using the EnKF and the RD-EnKF (perfect model). The right panels show the RMSE and Spread for both schemes under imperfect modeling conditions. Spatially and temporally averaged prior inflation values for each run are also shown.



Figure 5: Rank histograms for unobserved variable #32 obtained using the EnKF and the RD-EnKF (perfect model). The right panels show the RMSE and Spread for both schemes under imperfect modeling conditions. Spatially and temporally averaged prior inflation values for each run are also shown.



Figure 5: Rank histograms for unobserved variable #32 obtained using the EnKF and the RD-EnKF (perfect model). The right panels show the RMSE and Spread for both schemes under imperfect modeling conditions. Spatially and temporally averaged prior inflation values for each run are also shown.



Figure 5: Rank histograms for unobserved variable #32 obtained using the EnKF and the RD-EnKF (perfect model). The right panels show the RMSE and Spread for both schemes under imperfect modeling conditions. Spatially and temporally averaged prior inflation values for each run are also shown.



Figure 5: Rank histograms for unobserved variable #32 obtained using the EnKF and the RD-EnKF (perfect model). The right panels show the RMSE and Spread for both schemes under imperfect modeling conditions. Spatially and temporally averaged prior inflation values for each run are also shown.



Figure 5: Rank histograms for unobserved variable #32 obtained using the EnKF and the RD-EnKF (perfect model). The right panels show the RMSE and Spread for both schemes under imperfect modeling conditions. Spatially and temporally averaged prior inflation values for each run are also shown.



Figure 5: Rank histograms for unobserved variable #32 obtained using the EnKF and the RD-EnKF (perfect model). The right panels show the RMSE and Spread for both schemes under imperfect modeling conditions. Spatially and temporally averaged prior inflation values for each run are also shown.



Figure 5: Rank histograms for unobserved variable #32 obtained using the EnKF and the RD-EnKF (perfect model). The right panels show the RMSE and Spread for both schemes under imperfect modeling conditions. Spatially and temporally averaged prior inflation values for each run are also shown.



Figure 5: Rank histograms for unobserved variable #32 obtained using the EnKF and the RD-EnKF (perfect model). The right panels show the RMSE and Spread for both schemes under imperfect modeling conditions. Spatially and temporally averaged prior inflation values for each run are also shown.



Figure 5: Rank histograms for unobserved variable #32 obtained using the EnKF and the RD-EnKF (perfect model). The right panels show the RMSE and Spread for both schemes under imperfect modeling conditions. Spatially and temporally averaged prior inflation values for each run are also shown.



Figure 5: Rank histograms for unobserved variable #32 obtained using the EnKF and the RD-EnKF (perfect model). The right panels show the RMSE and Spread for both schemes under imperfect modeling conditions. Spatially and temporally averaged prior inflation values for each run are also shown.



Figure 5: Rank histograms for unobserved variable #32 obtained using the EnKF and the RD-EnKF (perfect model). The right panels show the RMSE and Spread for both schemes under imperfect modeling conditions. Spatially and temporally averaged prior inflation values for each run are also shown.



Figure 5: Rank histograms for unobserved variable #32 obtained using the EnKF and the RD-EnKF (perfect model). The right panels show the RMSE and Spread for both schemes under imperfect modeling conditions. Spatially and temporally averaged prior inflation values for each run are also shown.



Figure 5: Rank histograms for unobserved variable #32 obtained using the EnKF and the RD-EnKF (perfect model). The right panels show the RMSE and Spread for both schemes under imperfect modeling conditions. Spatially and temporally averaged prior inflation values for each run are also shown.



Figure 5: Rank histograms for unobserved variable #32 obtained using the EnKF and the RD-EnKF (perfect model). The right panels show the RMSE and Spread for both schemes under imperfect modeling conditions. Spatially and temporally averaged prior inflation values for each run are also shown.



Figure 5: Rank histograms for unobserved variable #32 obtained using the EnKF and the RD-EnKF (perfect model). The right panels show the RMSE and Spread for both schemes under imperfect modeling conditions. Spatially and temporally averaged prior inflation values for each run are also shown.



Figure 5: Rank histograms for unobserved variable #32 obtained using the EnKF and the RD-EnKF (perfect model). The right panels show the RMSE and Spread for both schemes under imperfect modeling conditions. Spatially and temporally averaged prior inflation values for each run are also shown.



Figure 5: Rank histograms for unobserved variable #32 obtained using the EnKF and the RD-EnKF (perfect model). The right panels show the RMSE and Spread for both schemes under imperfect modeling conditions. Spatially and temporally averaged prior inflation values for each run are also shown.



Figure 5: Rank histograms for unobserved variable #32 obtained using the EnKF and the RD-EnKF (perfect model). The right panels show the RMSE and Spread for both schemes under imperfect modeling conditions. Spatially and temporally averaged prior inflation values for each run are also shown.



Figure 5: Rank histograms for unobserved variable #32 obtained using the EnKF and the RD-EnKF (perfect model). The right panels show the RMSE and Spread for both schemes under imperfect modeling conditions. Spatially and temporally averaged prior inflation values for each run are also shown.



Figure 5: Rank histograms for unobserved variable #32 obtained using the EnKF and the RD-EnKF (perfect model). The right panels show the RMSE and Spread for both schemes under imperfect modeling conditions. Spatially and tempor